PHYSICAL REVIEW E, VOLUME 65, 045301(R)

Flow of thin films on patterned surfaces: Controlling the instability

L. Kondic
Department of Mathematical Sciences and Center for Applied Mathematics and Statistics, New Jersey Institute of Technology, Newark, New Jersey 07102

J. Diez
Instituto de Física Arroyo Seco, Universidad Nacional del Centro de la Provincia de Buenos Aires Pinto 399, 7000, Tandil, Argentina

(Received 27 July 2001; published 8 April 2002)

We present fully nonlinear time-dependent simulations of the gravity-driven flow of thin wetting liquid films. The computations of the flow on a homogeneous substrate show that the contact line, becomes unstable and develops a fingerlike or sawtooth structure [Phys. Rev. Lett. **86**, 632 (2001)]. These computations are extended to patterned surfaces, where surface heterogeneities are introduced in a controllable manner. We discuss the conditions that need to be satisfied so that surface properties lead to predictable pattern formation and controllable wetting of the substrate. These conditions are sensitive to the presence of noise which is introduced by random perturbations of the contact line. We analyze this sensitivity and suggest how the effects of noise can be minimized. Applications of these results to technologically relevant flows are discussed.

DOI: 10.1103/PhysRevE.65.045301 PACS number(s): 47.15.Gf, 47.20.Ma, 47.62.+q, 68.15.+e

In a number of technological applications, the contact line of a thin film spreading on a solid surface becomes unstable, leading to the formation of rivulets of fingerlike or triangular shape, and uneven surface coverage. In coating processes these instabilities are unwelcome since they may lead to the formation of dry regions. In other applications, such as those related to microfluidic devices, one desires to produce a partially wetted substrate. An example is provided by recent experiments [1], where an imposed surface anisotropy in the form of regularly spaced strips leads to regular patterns in the flow driven by thermocapillary stresses.

In this paper, we concentrate on perhaps the simplest of unstable thin-film flows, namely, the gravity-driven flow of a wetting fluid down an inclined plane. This configuration retains the most important aspects of the problem, while its relative simplicity allows for detailed theoretical and computational analysis. One hopes that if this problem can be understood in detail, the analysis can be extended to more complex driving forces, fluids, or flow geometries. Further, the main results are scale independent, allowing for rescaling of macroscopic simulations to micro- or even shorter scales.

The basic scenario for the instability development is that after the release, the initially straight contact line becomes unstable with respect to transverse perturbations. The essential characteristics of the initial stage of instability are explained by linear stability analysis (LSA) [2–4], which shows that the competition between stabilizing surface tension and destabilizing gravity leads to a band of unstable modes. Intuitive understanding of this instability can be reached by realizing that the balance of the forces generates a capillary ridge behind the moving front. This ridge can be thought of as a local accumulation of gravitational potential energy which is released by development of transverse structures (fingers or triangles) in the manner which is not dissimilar to Rayleigh-Taylor instability. LSA results are basically supported by experiments, although there are still open issues regarding instabilities for very small inclination angles [4,5]. Some aspects of the effect of inclination angle on instability are reported in our previous works [6]. Here we consider the influence of surface heterogeneity, with particular emphasis on the flow on patterned surface and resulting selective wetting. For brevity, we discuss only the flow down a vertical plane.

Within the lubrication approximation, the flow is the result of the balance among viscous, gravity and capillary forces. Its velocity $\mathbf{v}$ averaged over the normal direction z for an incompressible fluid is given by (e.g., [7,8])

$$3\mu\mathbf{v}=\gamma h^2\boldsymbol{\nabla}\nabla^2 h+\rho g h^2, \tag{1}$$

where μ is the viscosity, γ is the surface tension, ρ is the density, $h=h(x,y,t)$ is the fluid thickness, and $\nabla=(\partial_x,\partial_y)$ (x points downward and y is in horizontal transverse direction). By using this expression in the mass conservation equation, $\partial h/\partial t+\boldsymbol{\nabla}\cdot(h\mathbf{v})=0$, we obtain the following dimensionless partial differential equation

$$\frac{\partial h}{\partial t}+\boldsymbol{\nabla}\cdot[h^3\boldsymbol{\nabla}\nabla^2 h]+\frac{\partial h^3}{\partial x}=0. \tag{2}$$

Here, thickness h and coordinates x, y are expressed in units of h_0 (the fluid thickness far behind the front), and $\ell=h_0 Ca^{-1/3}$, respectively. The capillary number $Ca=\mu U/\gamma$ is defined in terms of the flow velocity U far behind the front. The time scale is chosen as ℓ/U, i.e., the approximate time it takes the contact line to advance a distance ℓ. Although Ca does not appear explicitly in Eq. (2), we define it here to point out the limits of the lubrication approximation, which holds provided Ca is small. Regarding boundary conditions, we concentrate on the problem where fluid thickness h_0 is kept constant. For later reference, note that LSA of Eq. (2) shows that the band of unstable modes is characterized by the wavelength of maximum growth $\lambda^*\approx 14$, and the marginally stable wavelength, $\lambda_c\approx 8$ [2].

All the theoretical and computational methods require some regularizing mechanism at the contact line [9]. One approach is to relax the no-slip boundary condition [7,9]; another one is to introduce a small foot of fluid, called precursor film, in front of the apparent contact line [2,4]; similarly, one can assume that the surface is prewetted. Recent computations [10] show, in agreement with previous works (e.g. [3]), that the choice of a regularizing model does not significantly effect the dynamics of the fluid as a whole. What *does* influence the dynamics is the introduced length scale; thinner precursor/slipping length b leads to increased energy dissipation and slows down the flow. Note that LSA and recent experiments [5] have also shown that smaller b's lead to increased instability with respect to transverse perturbations.

Since our goal is to understand the flow on patterned surfaces, and we already have a parameter b that measures the resistance to the flow, it is reasonable to consider modeling the surface features by allowing for spatially dependent b. While it might appear that imposing perturbations of this form is rather restrictive, this approach is actually quite general. The main idea is to impose heterogeneity on the system, and, since the macroscopic behavior of the film is not very sensitive to the microscopic details, the exact manner in which this is done is not crucial. As pointed out above, the introduced length scale determines the degree of energy dissipation at the front, and one expects that its spatial variation can have significant influence on the macroscopic flow properties [11]. We note that a similar method was used to model effects of surface noise [12]. We also note that our simulations are complementary to the works which analyze the flow over perturbations whose depth is comparable to film thickness [13]; the perturbations considered here are on the scale of b, i.e., much smaller than the thickness of the main body of the film.

Our computational methods, including discussion of efficiency, convergence, and accuracy are presented elsewhere [6,10]. Briefly, we use a finite difference method coupled with implicit Crank-Nicolson scheme. Boundary conditions simulate constant influx of the fluid, and at the y boundaries we impose Neumann-type conditions that lead to zero flux there; these boundaries can be thought of as slipping walls, or as symmetry planes. The simulations that follow use up to 60 000 grid points, leading to a large system of nonlinear algebraic equations to be solved at each time step; correspondingly, computational efficiency is crucial. For this reason, we use a precursor film model, which is computationally much more efficient [10].

Figure 1 shows an example of our results. At $t=0$ we start the evolution from the initial condition obtained in one-dimensional (1D) simulations that assume y independence. The flow is uniform until it reaches the imposed "channels" at $x_c=10$ in the flat precursor of thickness b_0. These channels have a flat central region of depth δb_0 ($\delta<1$), and a surrounding transition region, specified by $b(y)=b_0[1-\delta\exp(-w_t(y-y_c)^2)]$, where w_t denotes the transition width, and y_c is where the flat and transition regions meet. The results are insensitive to the choice of the specific function $b(y)$, or to w_t; we typically use $w_t=4$. Below, we report the

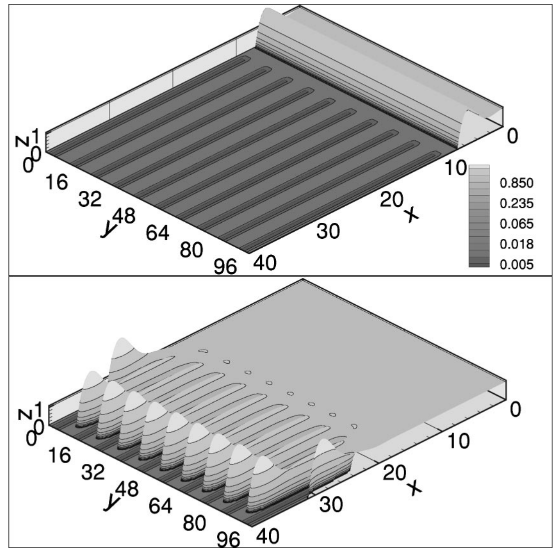

FIG. 1. Contour plot of the flow over a striped substrate. (a) Initial configuration (the straight contact line is at $x=7$). (b) Well-developed fingers propagating between the channels. The width of the channels is $w=3.5$, the distance between their centers is $d=10$, and they are imposed at $x_c=10$. Note that $y=48$ is a symmetry line; $b_0=0.01$.

distance d, between the centers of the channels, and their effective width w, defined as the width of the region where b is less than $b_0(1+\delta)/2$.

Since there is more resistance to the flow in the channels (where b is smaller), the fluid preferentially flows in the "easy" flow regions in between the channels. As a result, finger-like patterns form, characterized by the formation of a characteristic capillary ridge at the tips [see Fig. 1(b)]. These patterns are similar to those seen in the experiments [14] and also in the simulations where contact line itself is perturbed [6].

A significant difference, however, is that the position and the distance between the emerging patterns is predetermined by the imposed channels. In the particular case shown in Fig. 1, this distance is equal to 10, significantly less than λ^* predicted by LSA, or the one (≈ 12) observed in the experiments [14] and the simulations [6]. Therefore, one can use the channels to squeeze the emerging fingers closer together, as in experiments [1].

The experiments have also shown that there are limits to how closely the fingers can be made to flow [1]. Figure 2(a) ($d=8$) shows that in simulations the fluid still follows the surface features; however, in $d=7$ case [Fig. 2(b)], this is not the case anymore. Here, $d<\lambda_c$ is too small to force the fluid along the surface features (surface tension prevents such large curvature between fingers). The contact line does, however, become unstable, and develops fingers characterized by nonuniform separations and growth rates, similarly to experiments [1]. In the simulations, this instability is induced by the broken periodicity of the channel configuration ($d\neq 7$ close to $y=0$ and $y=96$), which represents a *long* wavelength perturbation. On the other hand, for $d=6$ [Fig. 2(c)], the periodicity is satisfied, and therefore, the contact line remains flat [small oscillations barely visible in Fig. 2(c), occur on the grid scale and disappear under grid refine-

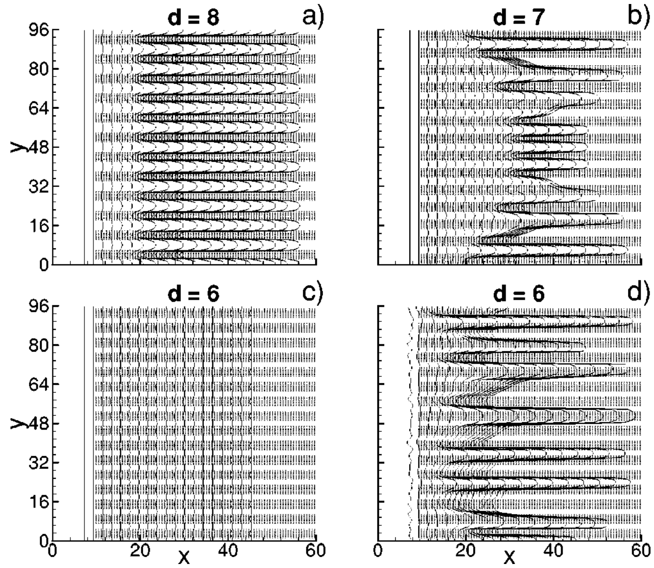

FIG. 2. Snapshots of the fluid profiles in $\delta t=2$ intervals. Shaded regions represent the channels. All parameters (except d's) are as in Fig. 1. In (d) the initial position of the contact line is perturbed by random noise (see text).

ment]. Similarly to $d=7$ case, capillary forces prevent the fluid from following the *short* wavelength imposed by the surface features.

This configuration characterized by a flat contact line has not been observed experimentally. Figure 2(d) shows that the reason is that this solution is unstable to small perturbations (noise). Here, we perturb the initial straight contact line at $t=0$ by small random perturbations (see below for details); this is sufficient to induce instability. Additional simulations have shown that *any* perturbation captured by numerical resolution is sufficient to induce instability. Therefore, we conjecture that small perturbations of either the contact line or the channels configuration can lead to the experimentally observed instability [1] for $d<\lambda_c$.

What happens if the distance between the channels is large compared to λ_c? From the simulations on uniform surfaces, we know that if the contact line is perturbed by long wavelengths, superharmonic frequencies can be excited through nonlinear mode (self) interaction [6]. Naturally, one expects a similar effect here. Indeed, Fig. 3 shows that this is exactly what happens. In Fig. 3(a) ($d=20$) we observe the beginning of excitations of modes characterized by shorter

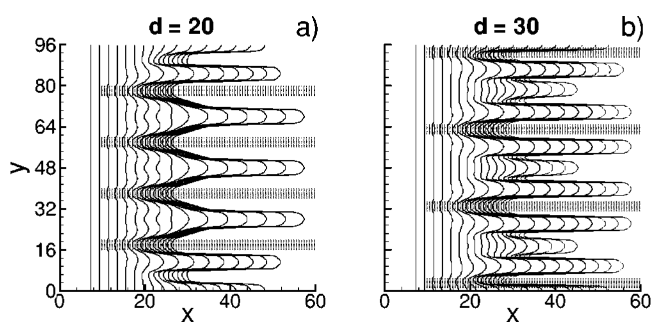

FIG. 3. Fluid profiles for large distances between channels.

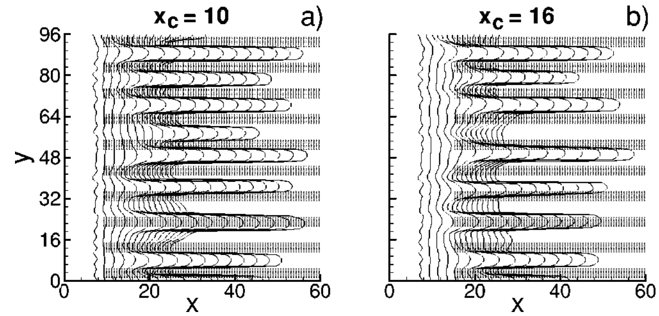

FIG. 4. Snapshots of the flow where the contact line is perturbed at $t=0$ by $N=50$ modes characterized by random amplitudes A_i, $|A_i|\leqslant 0.1$. Here, $d=10$; compare with Fig. 1 for the case without perturbations.

wavelengths; however, channels suppress this instability. The result is that there is still a single finger in each easy flow region, except at the sides of the domain, where there is more space. In contrast, $d=30$ (Fig. 3b) leaves enough space for three fingers in each of the easy flow regions. Interestingly enough, initially only two fingers develop, and than "secondary" instability leads to the third one. A possible explanation is that the channels first locally perturb the flow and induce instability in their vicinity; for longer times additional finger forms, since the distance between primary ones is large enough. To our knowledge, these patterns have not yet been observed experimentally.

There are other parameters that influence the instability mechanism and pattern formation: unperturbed precursor thickness, the depth and the relative width of the imposed channels, as well as the inclination angle of the plate. Although the effects of these parameters are rather interesting, here we concentrate on another question, and that is the influence of noise.

We model noise by perturbing the contact line at $t=0$ by a set of $N\gg 1$ modes, characterized by random amplitudes and wavelengths $\lambda_i=2L_y/i$, $i=1,\ldots,N$ [6]. These random perturbations grow rather quickly and develop patterns which are typically inconsistent with the channel distribution. A relevant question is how to avoid that these random perturbations prevent the fluid from following the pattern imposed on the precursor film.

Figure 4(a) shows the resulting patterns for $d=10$, with $x_c=10$ (as in the previous figures). We see that the contact line perturbations are strong enough to prevent the fluid from following the channels consistently (compare with Fig. 1), although most of the finger tips *are* in the easy flow regions. In Fig. 4(b), we take $x_c=16$, so that more time is left to the contact line perturbations to grow. In this case, the fluid follows the channels even less consistently, although there is a tendency of the evolving fingers to rearrange, so to flow in the easy regions. We note that the main features of the resulting flow are affected by noise only if it influences the flow significantly *before* it reaches the channel region; once the patterns are formed, we find very little sensitivity to noise. Additional simulations show that this general conclusion is insensitive to the particular noise realization, the maximum amplitude, or to the choice of d.

Quite generally, the influence of noise is to bring the system closer to its natural configuration. It breaks the symmetry introduced by the regular surface features, and may lead the system to a state different from the one with unperturbed precursor [Fig. 2(d) shows an extreme example]. We obtain this result for a gravity-driven flow down an inclined plane; however, due to the similarities of this system to more involved flows (driven by thermal, electric, or other forces), we expect this conclusion to be relevant to these other settings as well.

To summarize, in this paper we outline the connection between the natural instability of gravity-driven thin films on homogeneous surfaces, and the instability caused by imposed perturbations of the substrate. In the latter case, the shortest attainable distance between consecutive fingers is approximately equal to the critical wavelength λ_c obtained from LSA. Even in the relatively simple model where the strips are modeled by modified precursor thickness, we obtain results that are very similar to the flows where surface patterns are produced by spatially varying wetting properties [1].

Regularity of the flow may be modified by microscopic noise, which we model by perturbing the contact line. The main conclusion of practical relevance is that significant care has to be taken so that the natural instability does not interfere with the desired evolution of the wetting front. Our simulations show one way of reducing the effect of noise, and that is to decrease the distance between the release point and the channels region. Future research shall develop a more detailed understanding of the influence of noise on the flow on an inclined plane, as well as in other related thin-film systems.

J.D. acknowledges Fulbright Foundation, NJIT, and Consejo Nacional de Investigaciones Científicas y Técnicas (CONICET-Argentina) for supporting his visit to NJIT, and L.K. acknowledges support from NJIT Grant No. 421210.

[1] S.M. Troian, Nature (London) **402**, 794 (1999); A.A. Darhuber *et al.*, J. Appl. Phys. **88**, 5119 (2000).
[2] S.M. Troian *et al.*, Europhys. Lett. **10**, 25 (1989).
[3] M.A. Spaid and G.M. Homsy, Phys. Fluids **8**, 460 (1996).
[4] A.L. Bertozzi and M.P. Brenner, Phys. Fluids **9**, 530 (1997).
[5] Y. Ye and H. Chang, Phys. Fluids **11**, 2494 (1999).
[6] J. Diez and L. Kondic, Phys. Rev. Lett. **86**, 632 (2001); L. Kondic and J. Diez, Phys. Fluids **13**, 3168 (2001).
[7] H.P. Greenspan, J. Fluid Mech. **84**, 125 (1978).
[8] H. Huppert, Nature (London) **300**, 427 (1982).
[9] E.B. Dussan, J. Fluid Mech. **77**, 665 (1976); P.J. Haley and M.J. Miksis, *ibid.* **223**, 57 (1991).
[10] J. Diez, L. Kondic, and A.L. Bertozzi, Phys. Rev. E **63**, 011208 (2001).
[11] L. Kondic and A.L. Bertozzi, Phys. Fluids **11**, 3560 (1999).
[12] L.M. Hocking, J. Fluid Mech. **76**, 801 (1976); K. Hoffmann, B. Wagner, and A. Münch, in *Notes in Computational Science and Engineering*, Vol. 3, edited by H. J. Bungartz *et al.* (Springer-Verlag, Heidelberg, 1999).
[13] L.E. Stillwagon and R.G. Larson, Phys. Fluids A **2**, 1937 (1990); S. Kalliadasis, C. Bielarz, and G.M. Homsy, Phys. Fluids **12**, 1889 (2000).
[14] M. F. G. Johnson, PhD thesis, Northwestern University (1997).